Corrosion Resistance and Microstructure of Alumina-Magnesia Coating Material

TUNG-HSIN SU*, KUN-MING CHEN*, CHIH-YING LIU*, CHIA-HUNG KUO*, CHEN-SHIUN CHOU and YING-CHAO HUANG*****

**New Materials Research & Development Department, China Steel Corporation*
***Steelmaking Department, China Steel Corporation*
****Steelmaking Department, Dragon Steel Corporation*

The corrosion mechanism and microstructure of alumina-magnesia coating material were investigated based on the result of the rotary slag test. Analysis showed that a series of CaO-Al_2O_3 phases with low melting points was formed by the reaction between CaO in slag and Al_2O_3 in refractory, leading to the gradual dissolution of refractory in the slag. In-situ spinel ($MgAl_2O_4$) was formed during the rotary slag test. The result of the rotary slag test showed that samples with higher in-situ spinel had better slag resistance, whereas samples with pre-formed spinel had higher wear rates. Moreover, the addition of MgO with a coarser grain was found to restrict the formation of spinel and increase the apparent porosity of the refractory. On the contrary, the addition of sufficient fine-grained MgO could improve the in-situ spinel formation, thus effectively enhancing the corrosion resistance of the alumina-magnesia coating material.

Keywords: Alumina-Magnesia Coating Material, $Mgal_2o_4$ Spinel, Corrosion, Rotary Slag Test

1. INTRODUCTION

The alumina-magnesia coating material is used as a repairing material for the eroded areas of working linings in steel ladles. To extend the service life of working linings, the alumina-magnesia coating material must have good steel and slag resistance. The alumina-magnesia coating material is mainly composed of Al_2O_3 and MgO, where fused corundum is used as aggregate and alumina, magnesia, calcium aluminate cement, silica, fiber, and various additives as a matrix. During service, magnesia reacts with alumina to form in-situ spinel at temperatures above 1200°C. According to Wagner's mechanism, the solid-state spinel formation is carried out through the diffusion of Al^{3+} and Mg^{2+} ions at the MgO-$MgAl_2O_4$ and Al_2O_3-$MgAl_2O_4$ interfaces[1-3]. To keep the electro-neutrality, 3 Mg^{2+} ions diffuse to the alumina side whereas 2 Al^{3+} ions to the magnesia side. Since 3 Mg^{2+} generates 3 $MgAl_2O_4$ at the Al_2O_3 interface while 2 Al^{3+} forms only 1 $MgAl_2O_4$ at the MgO interface, the theoretical spinel formation rate is three times higher at the surface of Al_2O_3 than that of the MgO. Therefore, to achieve a better spinel-forming efficiency, a fine-grained MgO is preferred as the raw material for alumina-magnesia refractories. Owing to the increase in the specific surface area of MgO powder, the starting temperature of spinel formation reduces from 1200°C to 1000°C[3]. Since $MgAl_2O_4$ spinel has a lower coefficient of thermal expansion than MgO and a higher melting point than Al_2O_3[3, 4], spine-containing refractories often have superior thermal shock and corrosion resistance. Nowadays, Al_2O_3-MgO castable with either preformed or in-situ $MgAl_2O_4$ spinel is widely used as a working lining for steel ladles. Although castable with preformed spinel has better thermal resistance, the rotary slag test shows a better slag resistance for the in-situ spinel containing Al_2O_3-MgO castables[5]. Whether preformed or in-situ spinel formation provides better properties for Al_2O_3-MgO refractory remains controversial.

In this study, we aimed to investigate the corrosion mechanism of Al_2O_3-MgO coating material. Four alumina-magnesia coating materials were evaluated by the rotary slag test and their microstructures were analyzed.

2. EXPERIMENTAL METHOD

2.1. Sample Preparation

The alumina-magnesia coating materials were prepared by adding the appropriate amount of water (11-12%) and mixing for 3 minutes. The slurries were then poured into the mold and cured for 24hrs. After de-molding, the samples were dried in an oven at 110°C for 24 hours and prepared for the rotary slag test.

Samples for physical analyses were fired at 1500°C for 3 hours.

2.2. Test Methods

The constituent phase was identified by X-ray diffraction and composition was analyzed by X-ray fluorescence. The bulk density (BD) and apparent porosity (AP) were measured following JIS R2205 while cold crushing strength (CCS) and modulus of rupture (MOR) were tested using a universal testing machine (JIS R2553). The permanent linear change was analyzed following the procedure of JIS R2208. The corrosion resistance was evaluated using a rotating furnace. Each set of corrosion tests contained six samples which were arranged into a cylindrical chamber. During the test, a synthetic slag (CaO 48% 、MgO 8% 、Al_2O_3 25%, and SiO_2 19%) was introduced into the chamber and heated with a burner to 1600 °C. The cylindrical chamber was constantly rotating at 2 rpm, allowing molten slag to cover the sample surface. To enhance the corrosion speed, the synthetic slag was replaced six times every half hour. After the test, the wear rate was calculated by dividing the corroded depth by the original sample thickness. A smaller percentage represents better corrosion resistance. Microstructures of the reaction interface after the rotary slag test were analyzed by scanning electron microscopy (SEM) equipped with an energy dispersive spectrometer (EDS).

3. RESULTS AND DISCUSSION

3.1 Chemical Analyses and Physical Properties of Alumina-Magnesia Coating Material

The chemical composition and constituent phases of alumina-magnesia coating materials are listed in Table 1 and Figure 1. Based on the composition, the alumina-magnesia coating materials were separated into two groups: high (10.7 and 6.74% for samples A and D) and low MgO (2.65 and 3.32 % for samples B and C). Sample C had a higher CaO content (4.01%) than other samples (1.84-2.06%).

According to XRD analysis, the Al_2O_3 contents were contributed from corundum (Al_2O_3) and calcium aluminate cement ($CaAl_2O_4$) for all samples. Sample A, B, and D used periclase as a MgO source while sample C contained periclase (MgO) and spinel ($MgAl_2O_4$). The main constituent phases of all fired (1500°C/3hrs) samples were corundum, hibonite ($CaAl_{12}O_{19}$; CA6), and spinel (Figure 2). The dominant phase of sample A was spinel while others were corundum. Since sample A had the highest MgO content (10.7%; Table 1), more spinel was expected to form under high temperatures. Sample C has a relatively high CaO content, which indicates a higher cement addition in the raw material. This led to higher hibonite contents from the reaction of cement and Al_2O_3 during firing.

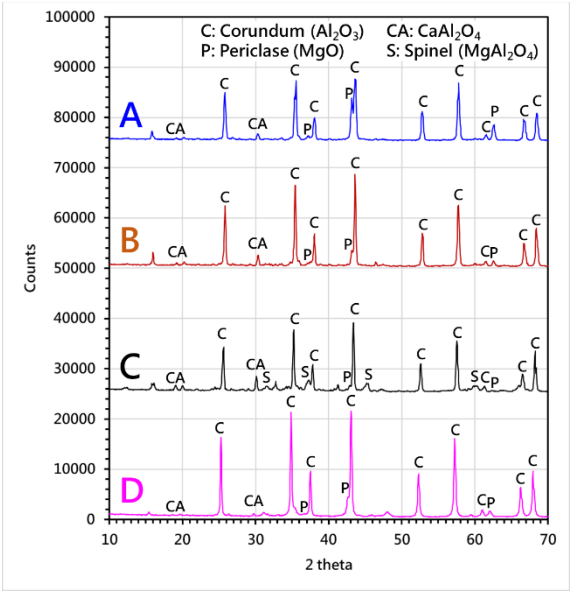

Fig.1. XRD analysis of the alumina-magnesia coating materials.

The physical properties of alumina-magnesia coating material after being fired at 1500°C for 3 hours are given in Table 2. Sample C had relatively low cold crushing strength and modulus of rupture, while its apparent porosity and permanent linear change were significantly higher than other samples. Such a distinct character was attributed to the addition of preformed spinel in sample C (Figure 1).

Table 1 Chemical composition of alumina-magnesia coating materials.

Wt.%	MgO	Al_2O_3	CaO	SiO_2
A	10.7	85.1	1.84	1.82
B	2.65	93.3	2.06	1.67
C	3.32	88.8	4.01	1.50
D	6.74	88.9	1.93	1.62

Table 2 Physical properties of alumina-magnesia coating materials after fired at 1500°C for 3 hours.

	Bulk Density (g/cm^3)	Apparent Porosity (%)	Cold Crushing Strength (MPa)	Modulus of Rupture (MPa)	Permanent Linear Change (%)
A	2.58	29.3	79.5	23.4	-0.04
B	2.66	29.3	29.7	11.9	-0.34
C	2.32	39.0	13.1	5.2	2.53
D	2.75	27.2	51.4	17.8	-0.78

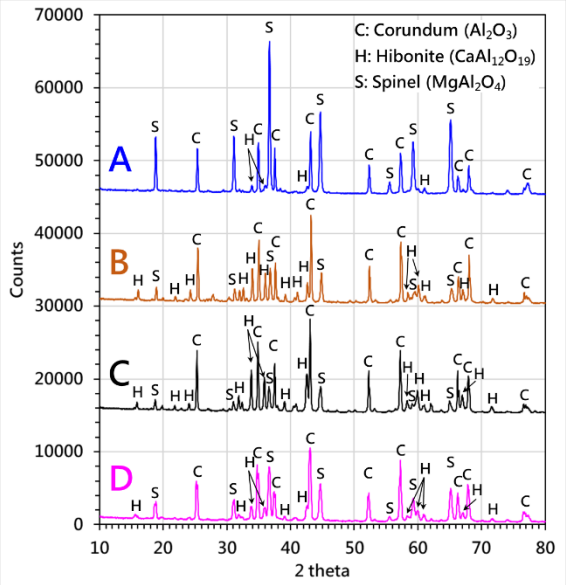

Fig.2 XRD analysis of alumina-magnesia coating materials after fired at 1500°C for 3 hours.

3.2 Corrosion Resistance of Alumina-Magnesia Coating Materials

The results of the rotary slag test are shown in Figure 3, where the slashed area, thick black line, and dashed lines indicate the corroded area, a crack that penetrates through the samples, and a small crack, respectively. It can be seen that alumina-magnesia coating materials with higher MgO contents (samples A and D) had low wear rates (14.6 and 12.9%) whereas other samples with lower MgO contents had poor corrosion resistance (sample B: 19.2%; sample D: 19.5%). XRD analysis showed that more spinel was formed in samples A and D (Figure 2), suggesting the existence of in-situ spinel could enhance the slag resistance of alumina-magnesia coating material. Note that in samples A and B, cracks developed parallel to the slag/refractory interface, leading to severe structural spalling (Figure 3). Although sample A showed a lower wear rate than sample C, the existence of structure spalling would likely result in a poorer performance of sample A than sample C in the field.

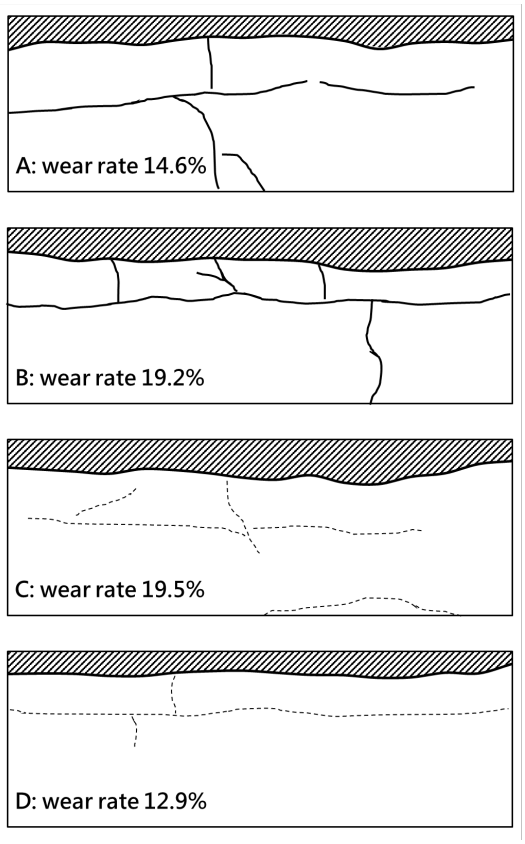

Fig.3. Schematic longitudinal cross-sectional drawings of alumina-magnesia coating materials after rotary slag test. The slashed areas indicate the corroded parts with wear rate in percentage given in each sketch. Thick black lines are big cracks that penetrate through samples while dash lines are small cracks where the material remains undivided.

3.3 Petrographic Study and Interpretation

To better understand the corrosion mechanism of alumina-magnesia coating material, a thorough petrographic investigation was conducted to study the phases and microstructures of the interface between the slag and the refractory. As illustrated in Figure 4, the interface can be divided into three regions: refractory, slag penetrated/corroded region and molten slag region. A dense layer of in-situ $MgAl_2O_4$ spinel was found in the interface.

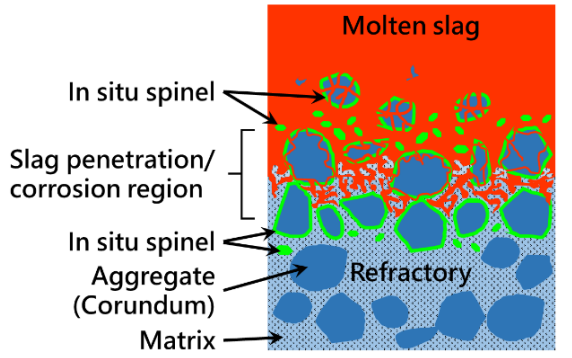

Fig.4. Schematic illustration of the slag/refractory interface. According to the extent of slag penetration, the slag/refractory interface can be further divided into refractory region (slag free), slag penetrated/corroded region, and molten slag region, respectively.

In the refractory region of sample A (Figure 5A), the matrix of alumina-magnesia coating material remained porous and the shape of aggregates (corundum) was angular. Both features indicate that the refractory region was not penetrated or corroded by slag. However, microprobe analysis shows that a thin layer of $MgAl_2O_4$ spinel was formed around the corundum aggregates (Figure 5B). This $MgAl_2O_4$ spinel was formed during the rotary slag test when the temperature of the refractory increased to > 1200°C [3]. Since $MgAl_2O_4$ spinel (2135°C) has a higher melting point than corundum (2054°C), this spinel layer would likely protect the corundum aggregate and increase its slag resistance.

In the slag-penetrated/corroded region of sample A (Figure 6A), the porosity was significantly reduced by slag penetration. Numerous euhedral $MgAl_2O_4$ spinel and $CaAl_{12}O_{19}$ were crystallized in the matrix of alumina-magnesia coating material. The surface of the corundum aggregate was corroded by slag and exhibited a more rounded appearance. Microprobe analysis showed that the corundum aggregates in the slag penetrated/corroded region was covered firstly by $CaAl_{12}O_{19}$ and then a layer of $MgAl_2O_4$ spinel (Figure 6B). During the rotary slag test, when the molten slag penetrated the alumina-magnesia coating material, the CaO from the synthetic slag would react with Al_2O_3 to form $CaAl_{12}O_{19}$. Therefore, $CaAl_{12}O_{19}$ was found in the matrix and on the surface of the corundum aggregate. EDS analysis showed that after reacting with refractory, the CaO content of the synthetic slag decreased from that (A) corundum aggregate was corroded and (B) euhedral 48% to ~37% while the Al_2O_3 content increased from 25% to ~36%. In the SiO_2-CaO-MgO-Al_2O_3 system, the primary field of spinel expands significantly when the Al_2O_3 content increases from 25% to 35% (Figure 7A).

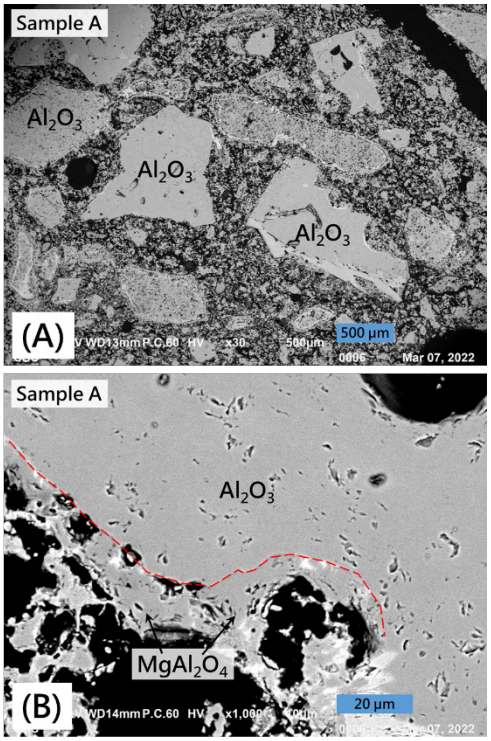

Fig.5. BEI (Backscattered Electron Image) images of (A) angular corundum aggregates and porous matrix in the refractory region, and (B) in-situ MgAl2O4 spinel layer formed on the surface of corundum aggregate.

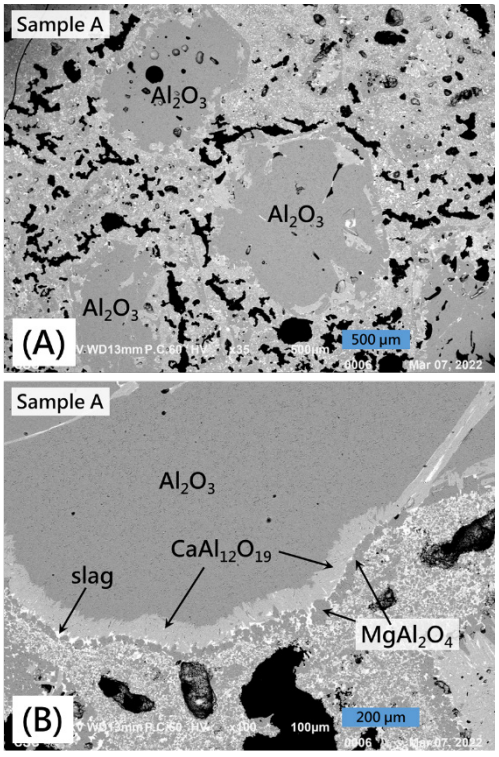

Fig.6. BEI images of slag penetrated/corroded region show $MgAl_2O_4$ spinel and $CaAl_{12}O_{19}$ was crystallized in the matrix and on the surface of corundum aggregate.

This compositional change in synthetic slag (Figure 7B) led to the crystallization of MgO-Al_2O_3. Thus, a layer of $MgAl_2O_4$ spinel was observed on the surface of $CaAl_{12}O_{19}$. Although the melting point of $CaAl_{12}O_{19}$ (~1730°C) is much lower than corundum, the two-layer structure of $CaAl_{12}O_{19}$-spinel still provided sufficient protection to the enclosed corundum aggregates, which increased the slag resistance for the alumina-magnesia coating material.

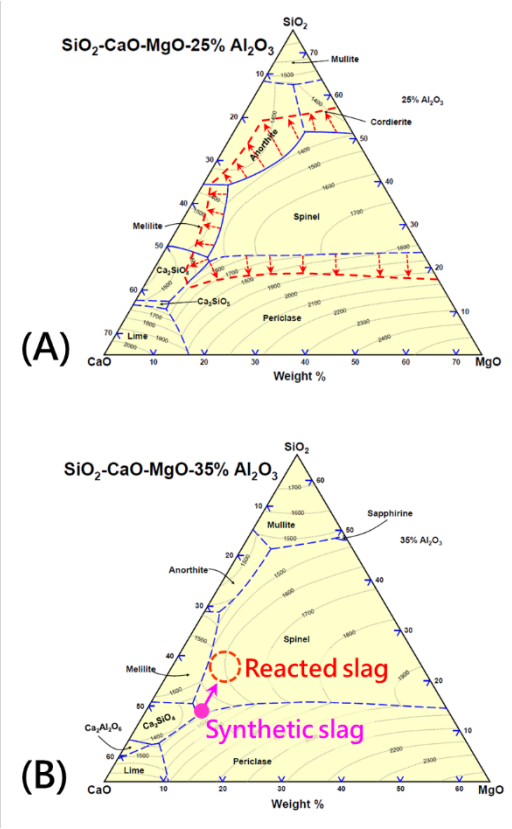

Fig.7. Phase diagram of SiO_2-CaO-MgO-Al_2O_3 system shows that (A) the primary field of spinel expanded when the Al2O3 content of the system increased from 25% to 35%, and (B) the composition of synthetic slag moved into the primary field of spinel.

Microscope observation showed that corundum aggregates were highly corroded in the molten slag region (Figure 8A). A low melting point (1595°C) phase, namely $CaAl_4O_7$ (CA2), was newly generated around the residual corundum aggregate and in the matrix. A considerable amount of euhedral $MgAl_2O_4$ spinel was also found in the slag/refractory interface (Figure 8B). There might be two origins of these spinels: (1) These spinels could be formed during heating or slag/refractory reaction, which would be easily eroded by hot metal or molten slag when the refractory is in service; (2) These spinels could be crystallized during the cooling process of the rotary slag test and had no effect for protection of refractory since they were formed after slag attacked.

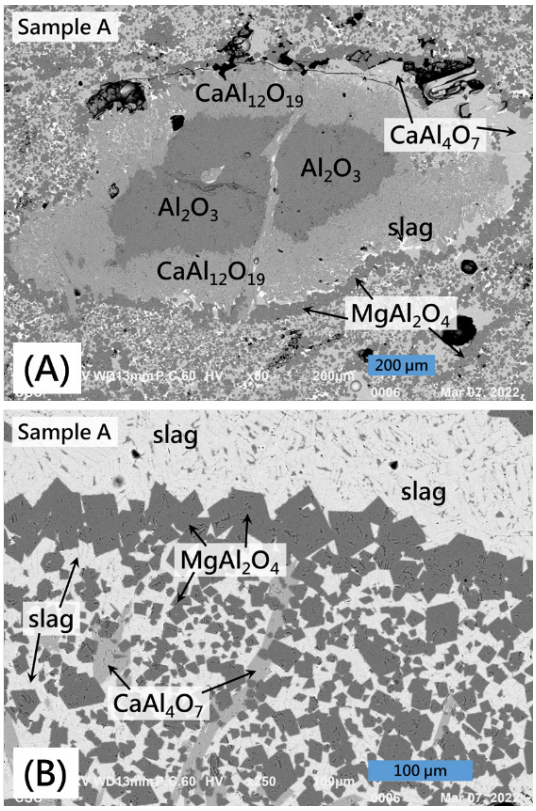

Fig.8. BEI images of the molten slag region show that (A) corundum aggregate was highly corroded and (B) euhedral $MgAl_2O_4$ spinel and $CaAl_4O_7$ were crystallized from the molten slag.

According to a previous discussion, there were three different mechanisms for the formation of in-situ $MgAl_2O_4$ spinel in alumina-magnesia coating material. (1) In the slag-free region of refractory, MgO reacted with Al_2O_3 directly to form $MgAl_2O_4$ spinel in the matrix or as a thin layer surrounding the corundum aggregates (Figure 9A). The source of MgO was provided by the refractory. (2) The slag-refractory reaction in the slag penetrated/corroded region, which has resulted in a compositional change of the synthetic slag to the primary field of spinel, induced the crystallization of $MgAl_2O_4$ spinel (Figure 7 and 9B). The MgO could be contributed from both the refractory and the synthetic slag. (3) Euhedral $MgAl_2O_4$ spinel crystallized directly from the molten slag near the slag/refractory interface (Figure 9C). The source of MgO was mostly from the molten-synthetic slag.

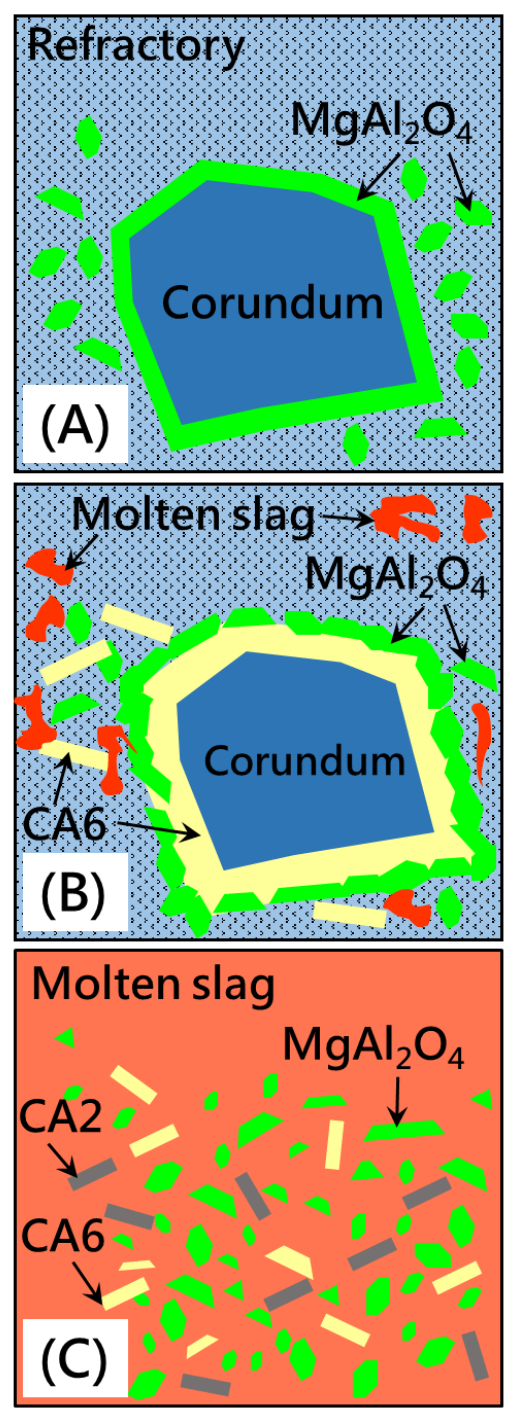

Fig.9. Schematic illustration of the microstructures from three different spinel-forming mechanisms including: (A) MgO reacts with Al_2O_3 directly to form $MgAl_2O_4$ spinel in the matrix and on corundum aggregate in the refractory region; (B) A sequential microstructure of corundum aggregate surrounded by CA6 and $MgAl_2O_4$ spinel layer in the slag penetration region; **(C)** Euhedral $MgAl_2O_4$ spinel, CA6 and CA2 crystallized directly from the molten slag.

EDS analysis showed that $MgAl_2O_4$ spinel formed by mechanisms (1) and (2) had an Al_2O_3/MgO ratio of 2.2-2.5, indicating a high alumina spinel crystallized in an alumina-rich environment. In contrast, $MgAl_2O_4$ spinel formed by mechanism (3) reached a stoichiometric balance with an Al_2O_3/MgO ratio of 2, which resulted from a relatively low Al_2O_3 environment of molten slag.

It was found that the slag resistance of alumina-magnesia coating material was highly correlated to the amount of in-situ spinel. Sample A and D, which contained more in-situ spinel in the refractory region, had better slag resistances. This could be attributed to the formation of an in-situ $MgAl_2O_4$ spinel layer, which was formed around the corundum aggregates before slag penetration. Meanwhile, the spinels in samples B and C were found mostly in the molten slag region, which had little effect on the improvement of slag resistance. With less spinel formed in the refractory and slag penetration region, the wear rates of samples B and C after rotary slag increased to 19.2 and 19.5%, which were significantly higher than that of samples A and D.

It is worth mentioning that sample C, which contained preformed spinel, had the worst slag resistance (Figure 1). This result coincided with the study done by Chen *et al*. in 2002, where Al_2O_3-MgO castables had better slag resistance than Al_2O_3-spinel castables based on rotary slag tests and field trials [5]. The slag resistance of alumina-magnesia coating material would benefit more from the well-bonded microstructure of in-situ $MgAl_2O_4$ spinel than that of the preformed $MgAl_2O_4$ spinel.

From the rotary slag test and microscope analyses, it was concluded that the corrosion mechanism of alumina-magnesia coating material was mainly initiated from the reaction between CaO in slag and Al_2O_3 (including corundum aggregate and Al_2O_3 powder in matrix) in refractory. A series of CaO-Al_2O_3 phases (CA6 and CA2) with increasing ratios of CaO/Al_2O_3, which corresponds to a decreasing melting point, were formed during the reaction [6]. Therefore, the aggregates and matrix of alumina-magnesia coating material were gradually corroded by slag. For samples with higher MgO contents (samples A and D), a sufficient amount of $MgAl_2O_4$ spinel was formed in the refractory region before slag penetration. The matrix and the corundum aggregate were protected by the $MgAl_2O_4$ spinel layer, resulting in a better slag resistance. Microscopic analysis also revealed the growth of CA6 crystals around the $MgAl_2O_4$ spinel in the bonding matrix of samples A and D (Figure 10). Chan and Ko, 1998 indicated that such an interlocking microstructure created a strong bond linkage between CA6 and spinel, leading to a higher hot strength[7]. This interlocking structure was absent in samples B and C since no sufficient spinel was formed in the refractory.

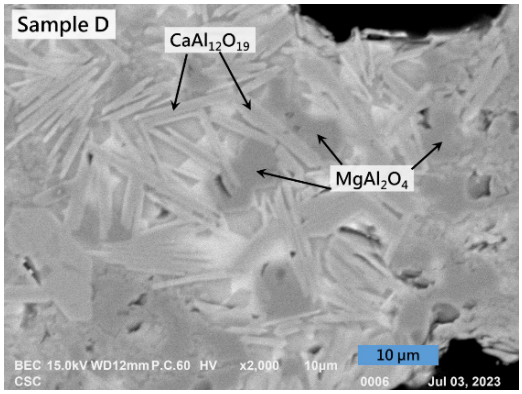

Fig.10. The interlocking microstructure of CA6 crystals growth around the $MgAl_2O_4$ spinel in the bonding matrix of sample D.

3.4 Influence of MgO Grain Size for the Formation of $MgAl_2O_4$ Spinel

No residual MgO was found in the slag/refractory interface after the rotary slag test in samples A, B, and D, suggesting that all MgO either became $MgAl_2O_4$ spinel or dissolved in the molten slag under high temperature. However, in the refractory and slag-penetrated/corroded regions of sample C, residual MgO particles with a grain size of ~1 mm were observed (Figure 11A). Microstructure analysis showed that a thick layer of $MgAl_2O_4$ spinel was formed around the residual MgO particles, separating them from Al_2O_3 and restricting the further formation of $MgAl_2O_4$ spinel. Therefore, only a little $MgAl_2O_4$ spinel was found in the matrix and no $MgAl_2O_4$ spinel was formed on the surface of corundum aggregates (Figure 11). Moreover, sample C had enormous pores (Figure 11B), which possibly resulted from the use of coarse-grained periclase as a MgO source to form spinel. It was found that the apparent porosity of sample C (39%) was 10% higher than other samples (27-29%; Table 2), which might have led to its poor slag resistance. Since the solid-state $MgAl_2O_4$ spinel formation was carried out through the Al^{3+} and Mg^{2+} ionic diffusion, the spinel formation rate should be three times higher at the surface of Al_2O_3 than MgO[1-3]. Therefore, the addition of fine-grained MgO could improve the in-situ spinel formation, thus effectively enhancing the corrosion resistance of the alumina-magnesia coating material.

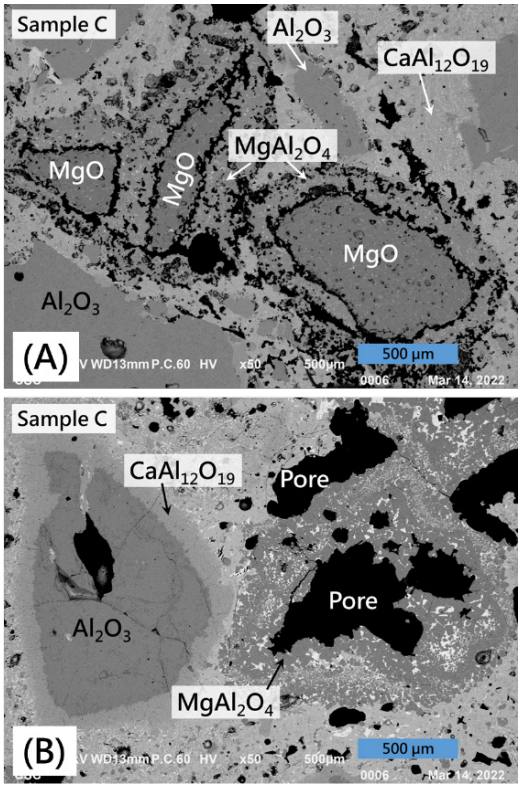

Fig.11. BEI images of (A) residual MgO particles, and (B) pores formed after residual MgO is completely consumed.

4. CONCLUSIONS

The corrosion resistance and microstructure of alumina-magnesia coating material were studied based on the rotary slag test. It was found that the CaO in slag and Al_2O_3 in refractory formed a series of CaO-Al_2O_3 phases (CA6 and CA2) with increasing ratios of CaO/Al_2O_3 and decreasing melting points, leading to the dissolution of the coating material. In-situ $MgAl_2O_4$ spinel, especially the ones that formed around corundum aggregates and created interlocking microstructures with CA6 in the matrix, provided a better slag resistance than that of the preformed spinel. Moreover, the addition of fine-grained MgO would enhance the formation of in-situ spinel, thus effectively increasing the corrosion resistance of the alumina-magnesia coating material.

REFERENCE

1. Nakagawa Z., Enomoto N., Yi I.S., Asano K., Effect of corundum/periclase sizes on expansion behavior during synthesis of spinel. Proceedings of UNITECR-1995 Japan, pp. 1312-1319, 1995.
2. Carter R.E., Mechanism of solid-state reaction between magnesium oxide and aluminum oxide and between magnesium oxide and ferric oxide, Journal of the American Ceramic Society, 44, pp. 116-120, 1997.
3. Braulio, M.A.L., Rigaud, M., Buhr, A., Parr, C., Pandolfelli, V.C., Spinel containing alumina-based refractory castables. Ceramics International, 37, pp. 1705-1724, 2011.
4. Tyrała, K., Ramult, J., Prorok, R., Madej, D., Influ-

ence of magnesium aluminate spinel on the thermo-mechanical properties of alumina-spinel castables. Proceedings of UNITECR-2019 Japan, pp. 269-273, 2019.
5. Chen, S.K., Cheng, M.Y., Lin, S.J., Ko, Y.C., Thermal characteristics of Al_2O_3-MgO and Al_2O_3-spinel castables for steel ladles, Ceramics International, 28, pp. 811-817, 2002.
6. Muan, A., Osborn, E.F., Phase equilibria among oxides in steelmaking. Addison-Wesley Publishing Company, Boston, 1965.
7. Chan, C.F., and Ko, Y.C., Effect of CaO content on the hot strength of alumina-spinel castables in the temperature range of 1000° to 1500°C. Journal of the American Ceramic Society, 81, pp. 2957-2960, 1998.